

Supporting Information

Fast acid-leaching strategy treated hollow cobalt-carbon materials as high-efficient electrochemical catalysts for Zn-air batteries

Jun Yang^a, Jilan Long^{a,*}, Cheng Chen^a, Guangming Liang^a, Bing Tang^a, Xiaohong Liu^b and Wei Zhang^{c,*}

^a Chemical Synthesis and Pollution Control Key Laboratory of Sichuan Province, College of Chemistry and Chemical Engineering, China West Normal University, Nanchong, 637000, PR China.

^b National University of Singapore (Chongqing) Research Institute, Chongqing 401123, P.R. China

^c Chongqing Institute of Green and Intelligent Technology, Chinese Academy of Sciences, Chongqing 400714, P. R. China

* Corresponding authors, e-mail: xlong612@126.com (J. Long);

andyzhangwei@163.com (W. Zhang).

Contents

1. Experimental section

2. Characterization

3. Experimental results

1. Experimental section

1.1 Electrochemical measurement for ORR and OER

The electrochemical performances of all catalysts were tested on a computer-controlled bipotentiostat (Princeton, PARSTAT 3000A-DX, USA) with three electrode systems with Pt/C as counter electrode, AgCl (for ORR) or Hg/HgO (for OER) catalysts as reference electrode, catalysts modified glassy carbon electrode (GCE) as work electrode. The synthetic procedure of work electrode is as follows: generally, 5mg catalyst was dispersed into 1 mL of EtOH-0.5wt% Nafion (v:v=9:1) solution and treated by ultrasonic processing. Then the polished glassy carbon electrode (GCE, diameter=5 mm) was modified by 10 uL of the catalysts ink to obtain a loading mass of 0.254 mg/cm². The CV and LSV tests were carried out in 0.1 M KOH with the scanning rate of 100 mV/s and 10 mV/s, respectively. After to test, all potentials were converted into reversible hydrogen electrode (RHE) according to the Nernst equation.

1.2 The assembly of liquid Zn-air battery

The liquid Zn-air battery is assembled with catalysts modified carbon paper as air cathode, Zn plates as anode, O₂-saturated 6M KOH as electrolyte. All of these components are fixed by a sealed battery model, while the cycling of electrolyte depends on a circulating pump connected with the sealed battery model. The synthetic procedure is as follows: in general, catalyst was dispersed into 300 uL of EtOH-nafion solution and treated by ultrasonic processing, then the catalysts ink were dipped onto the composite carbon paper (carbon paper+waterproof membrane+

conducting layer) to obtain a mass loading of 1 mg/cm² as air cathode catalysts.

1.3 The assembly of solid-state button Zn-air battery

The solid-state ZABs are assembled with catalysts modified carbon paper as air cathode, commercial Zn plate as anode, and PANa-KOH (sodium polyacrylate/6 M KOH; sodium polyacrylate purchases from Aladdin company) as electrolyte. The air cathode catalysts were prepared for the similar procedure of liquid ZABs, and the mass loading into catalysts was 1 mg/cm². Open circuit voltage, polarization curves, galvanostatic discharge curves and charge-discharge cycle curves were tested on the electrochemical workstation (Princeton, PARSTAT 3000A-DX, USA). As contrast, Pt/C-RuO₂(mass ratio 1:1) was also tested for the same conditions.

2. Characterization

The SEM and elemental mapping of Co@CN-P₁₀-750 catalysts and corresponding elements distribution were investigated with a scanning electron microscope (Zeiss, Gemini SEM 500). PXRD patterns of Co@CN-P₁₀-T catalysts were tested by a Rigaku diffractometer (Ultimal V, 3 kW) with Cu K α radiation (40 kV, 40 mA, 0.1543 nm). The Raman spectra were tested on the confocal microraman spectrometer (Witec alpha300 access, Germany). The XPS spectra of C, Co, N, S elements were measured on the X-ray photoelectron spectroscopy (XPS, Thermo Scientific ESCALAB 250Xi). The metal particles and morphology of the Co@CN-P₁₀-750 and Co@CN-P₁₀-750-H⁺(12h) catalysts were determined by a transmission electron microscope (TEM, JEOL, JEM-2010HR). The CV and LSV were measured

on the computer controlled electrochemical workstation (Princeton, PARSTAT 3000A-DX, USA) with a rotating disk electrode (Pine). The liquid and solid-state ZABs were also tested on the instrument of PARSTAT 3000A-DX.

3. Experimental results

Table S1. Chemical compositions of samples obtained from XPS results.

	P (atom%)	C (atom%)	N (atom%)	O (atom%)	Co (atom%)
Co@CN-P ₁₀ -700	0.88	74.5	6.52	14.35	3.75
Co@CN-P ₁₀ -750	0.82	77.06	5.71	13.06	3.35
Co@CN-P ₁₀ -800	0.63	80.24	4.39	10.02	4.72
Co@CN-P ₁₀ -850	0.52	81.61	4.02	8.02	5.83
Co@CN-P ₁₀ -900	0.25	84.97	2.89	5.24	6.65

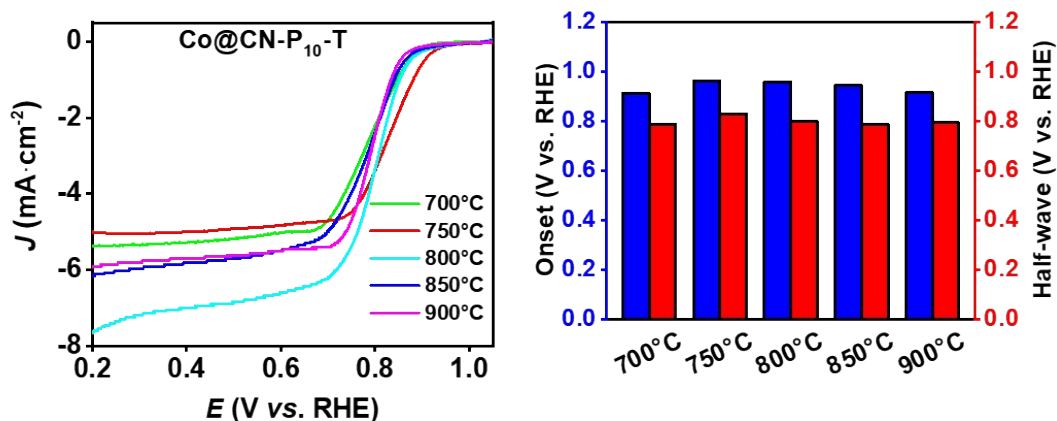


Fig. S1. (a) ORR performance of Co@CN-P₁₀ catalysts synthesized at different temperatures and (b) their performances comparison diagram.

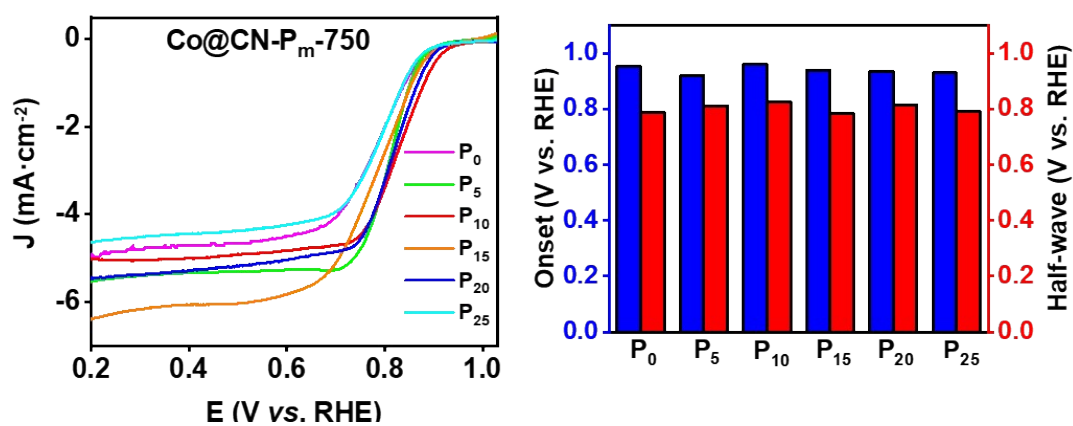


Fig. S2. (a) ORR performance of Co@CN-P_m-750 catalysts synthesized at 750 °C with different P contents in their template and (b) their performances comparison diagram.

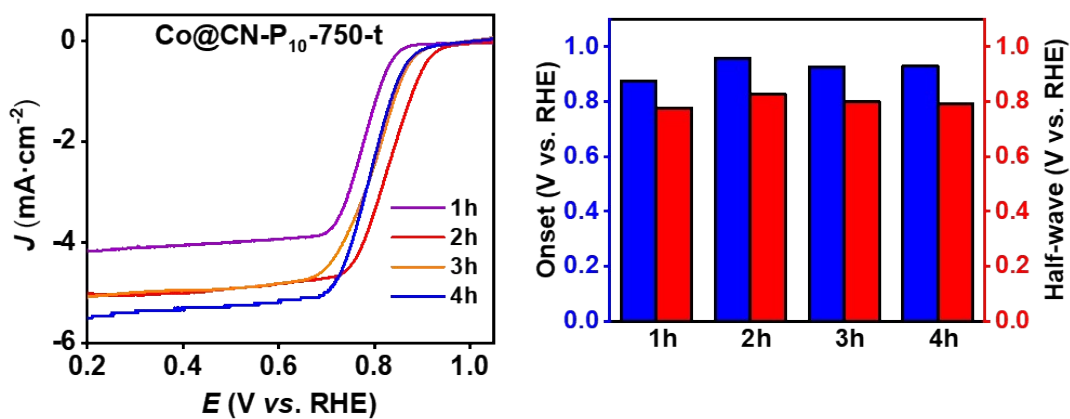


Fig. S3. (a) ORR performance of Co@CN-P₁₀-750 catalysts synthesized with various calcining time and (b) their performances comparison diagram.

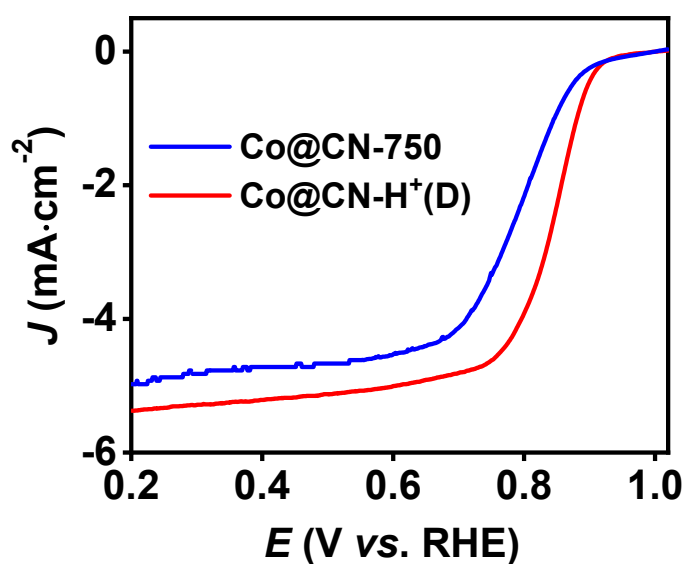


Fig. S4. The comparison of ORR performance of Co@CN-750 catalysts and its acid treatment products.

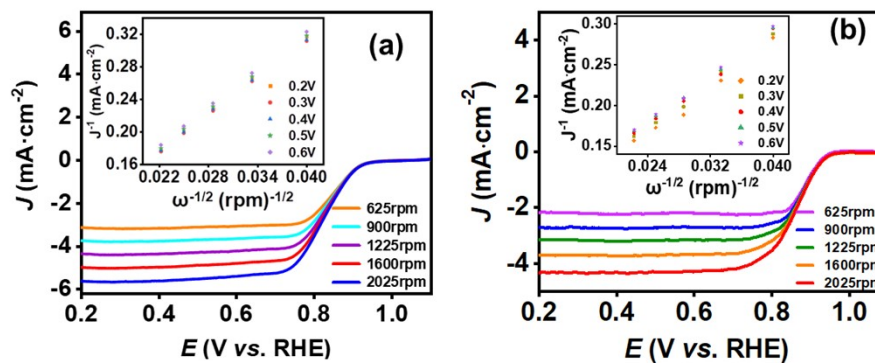


Fig. S5. The performances of fresh Co@CN-P₁₀-750-H⁺(D) and reused Co@CN-P₁₀-750-H⁺(D) catalysts after 9 h continuous i-t test.

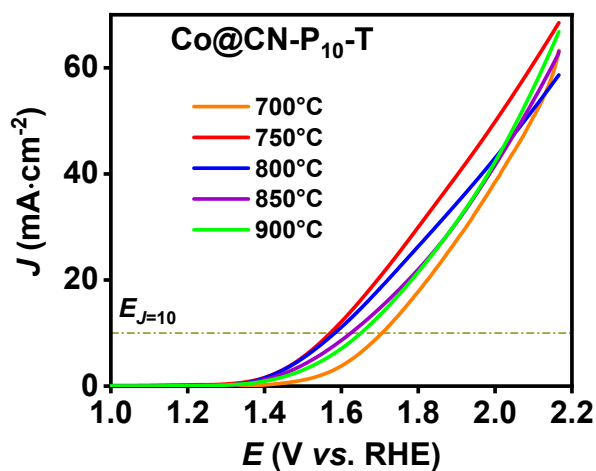


Fig. S6. OER performance of Co@CN-P₁₀ catalysts synthesized at different temperatures.

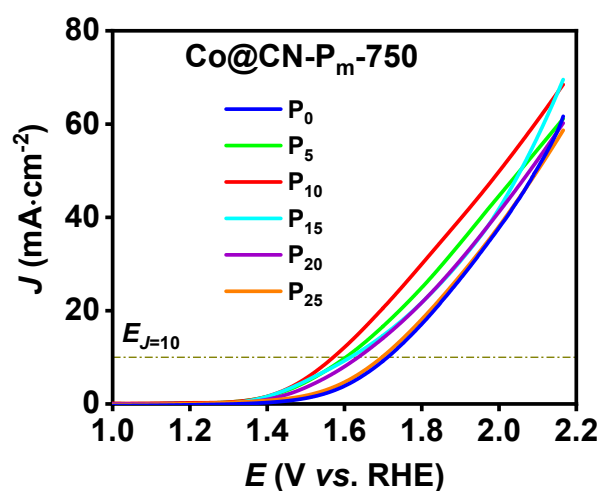


Fig. S7. OER performance of Co@CN-P_m-750 catalysts synthesized at 750 oC with different P-content templates.

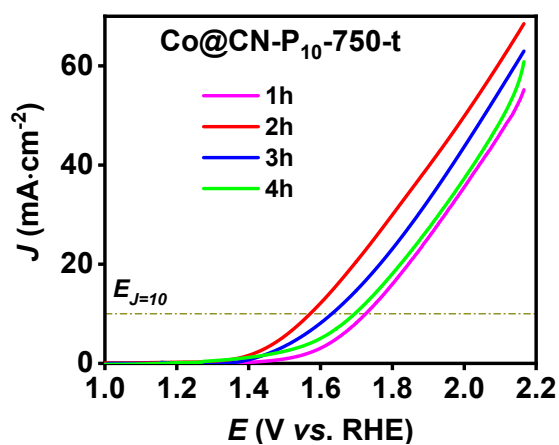


Fig. S8. OER performance of Co@CN-P₁₀-750 catalysts synthesized with different calcining time.

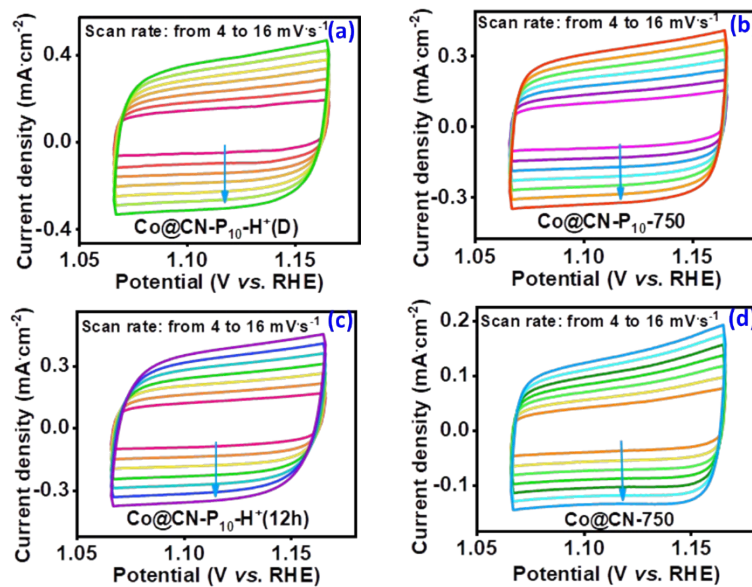


Fig. S9. CV curves of different catalysts. (a) Co@CN-P₁₀-750-H⁺(D), (b) Co@CN-P₁₀-750, (c) Co@CN-P₁₀-750-H⁺(12h), and (d) Co@CN-750.

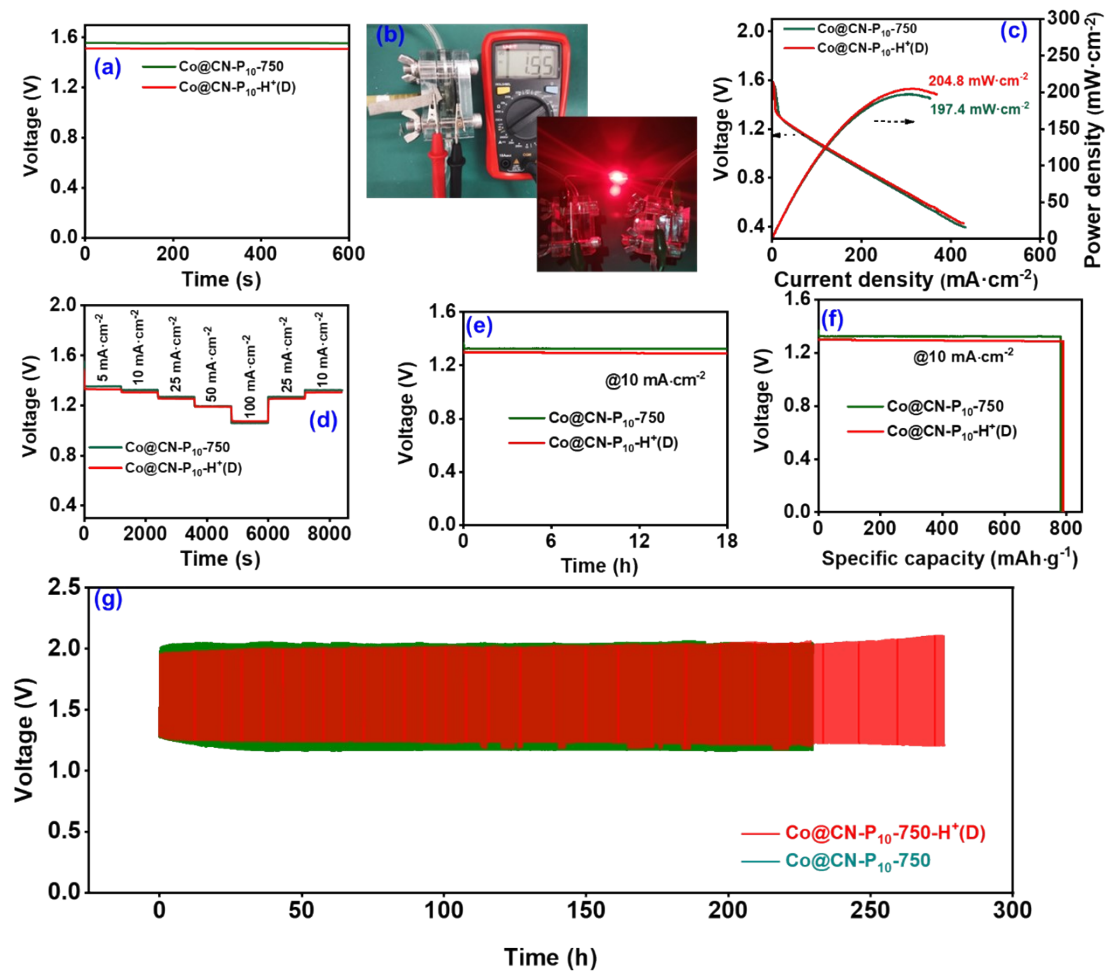


Fig. S10. (a) The OCV of home-made liquid ZABs assembled with different cathode catalysts, and (b) corresponding application schemes of Co@CN-P₁₀-750 based ZABs. (c) The maximum power density of ZABs, (d) rate performances of ZABs, (e) the discharge stability of ZABs at the current density of 10 mA/cm² and corresponding specific capacity (f). (g) The long-term charge-discharge curves of ZABs at the current of 2 mA/cm² with 20 minutes per cycle, and corresponding energy efficiencies (inset).

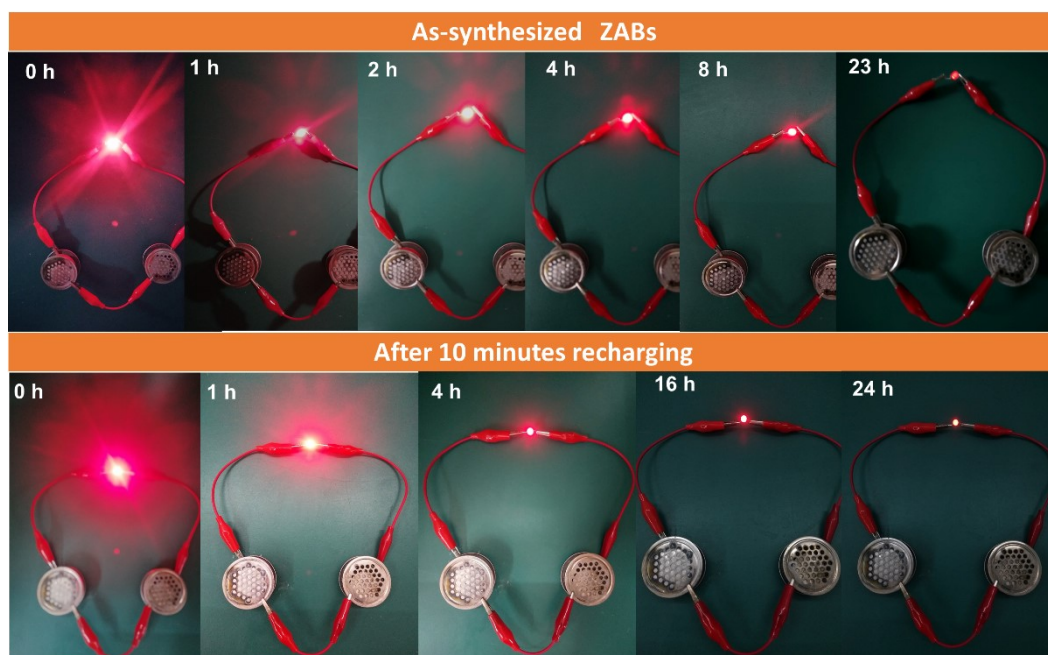


Fig. S11. The practical application of as-synthesized $\text{Co@CN-P}_{10-750-\text{H}^+(\text{D})}$ based solid-state ZABs, and the application of $\text{Co@CN-P}_{10-750-\text{H}^+(\text{D})}$ based ZABs after 10 minutes recharging at 10 mA/cm^2

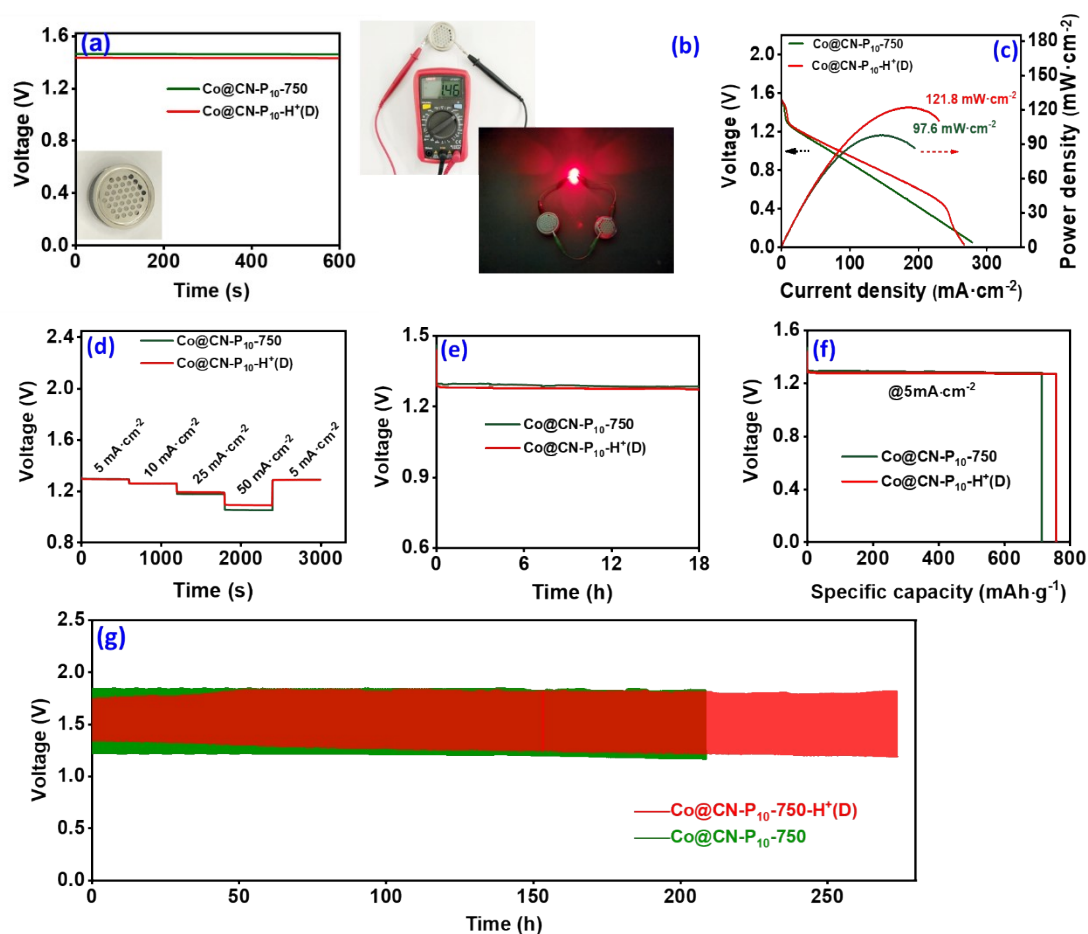


Fig. S12. (a) The OCV of home-made solid-state ZAB assembled with different catalysts, and (b) corresponding application images of Co@CN-P₁₀-750 based ZAB. (c) The maximum power density of ZABs, (d) rate performances of ZABs, (e) the discharge stability of ZABs at the current density of 5 mA/cm² and corresponding specific capacity (f). (g) The long-term charge-discharge curves of ZABs at the current of 1 mA/cm² with 20 minutes per cycle, and the energy efficiencies (inset).